

Modeling liquid migration in active swollen gel spheres

Michele Curatolo^{1, a)} Paola Nardinocchi^{1, b)} and Luciano Teresi^{2, c)}

¹⁾ *Sapienza, Università di Roma, Roma, Italy*

²⁾ *Università di Roma Tre, Roma, Italy*

(Dated: March 17, 2024)

Liquid migration in active soft solids is a very common phenomenon in Nature at different scales: from cells to leaves. It can be caused by mechanical as well as chemical actions. The work focuses on the migration of liquid provoked by remodeling processes in an active impermeable gel sphere. Within this context, we present a consistent mathematical theory capable to gain a deep understanding of the phenomenon in both steady and transient conditions.

PACS numbers: 46.05.+b, 81.05.Qk

Keywords: active swelling, liquid migration, turgor pressure

Active soft matter is the key constituent of living matter: its striking behavior is the capability of exploiting chemical energy to produce mechanical work, and thus move, morph and remodel. Cells are a prototypical example: their mechanical behavior is controlled by a network of crosslinked filaments which respond to energy-transducing molecular motors¹; the system is “out of thermodynamic equilibrium” and its functioning is based on the conversion of chemical power into mechanical power.

In the more recent years, the study of this kind of active system has been gaining an important role in both physics, as we need new experiments, and in mathematics, as we need new models². The present study focuses on a theory of active gels on the macroscale^{3–6} and aims to understand the mechanism under liquid redistribution which can be observed in active gels and in other macroscopic living systems where it delivers stresses affecting cell growth^{7–10}.

We use the perspective of continuum physics: an active gel is considered as a biphasic material consisting of an elastic polymer network bathed in an interstitial liquid. Activation produces a change in the mean free-lengths of the polymer chains: at the macroscale, this phenomenon is viewed as a change of the natural state of the network and named *material remodeling*. Liquid redistribution, network deformation and material remodeling are strongly coupled and affect one each other. They determine stresses within the gel which can alter material remodeling and gel shape and may drive further remodeling^{7,11,12}.

The state variables of the model, which is based on an augmented version of the classic Flory-Rehner thermodynamics for stress diffusion^{13,14} put within the framework of material remodeling,^{15–17} include remodeling variables: they describe the change in size and shape of volume elements due to the changes of the mean free-lengths of the polymer chains^{4,6} (see figure 1) As a secondary even if relevant effect, remodeling changes polymer network crosslink density too⁵. Lastly, active gels allow to discuss the interaction between liquid migration and stress generation which are so important in the remodeling of plant cells⁷.

Let us start from passive gels, swollen at equilibrium. A gel placed in a liquid changes its volume by absorbing or desorbing the liquid and eventually reaches thermodynamic equilibrium. Whenever constraint-free and under no loads, the equilibrium state of a homogeneous gel is stress-free, and its swelling is uniform. For example, a homogeneous gel sphere \mathcal{S}_d with dry-reference radius r_d (and dry-volume V_d) placed in a bath of chemical potential μ_o grows to get thermodynamical equilibrium and reaches a stress-free swollen state \mathcal{S}_o with radius $(J^{1/3})r_d$. The change in volume J is known from the chemical equilibrium equation which holds within the classic Flory-Rehner model of stress-diffusion

$$RT \left(\log \frac{J-1}{J} + \frac{1}{J} + \frac{\chi}{J^2} \right) + \frac{G}{J^{1/3}} \Omega = \mu_o, \quad (.1)$$

^{a)} michele.curatolo@uniroma1.it

^{b)} paola.nardinocchi@uniroma1.it

^{c)} luciano.teresi@uniroma1.it

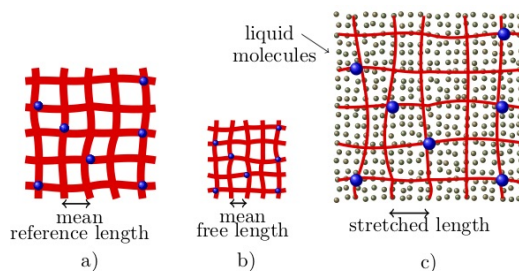


Figure 1. Three states of an active gel. a) Dry-reference state of the polymer network (red) with crosslinks (blue dots). b) Dry-remodeled (contracted) network: mean free-length is reduced and polymer chains are still un-stretched whereas the crosslink density changed. c) Swollen state: liquid molecules (brown dots) swell the dry-contracted network.

where R ([J/(K mol)]) is the universal gas constant, T ([K]) is the temperature, χ is the Flory parameter, G ([J/m³]) is the shear modulus of the dry gel, and Ω ([Ω] = m³/mol) is the molar volume of the liquid. The change in volume is equal to the liquid uptake: $J = 1 + \Omega c$, with c the liquid concentration per unit of dry volume ([mol/m³]). From now on we denote with J_o the change in volume from the dry to the swollen state \mathcal{S}_o . For $G = 10^4$ Pa, $\chi = 0.4$, $\Omega = 1.8 \cdot 10^{-5}$ m³/mol and $\mu_o = 0$ J/mol, $J_o = 77.6$, *i.e.* it corresponds to an increase of the original dry volume V_d of 77.6 times, due to liquid uptake (see cartoon in figure 2).

A further change of the environmental conditions, both mechanical and chemical, drives the gel to a new equilibrium state \mathcal{S} and determines a further change in volume. For example, liquid is expelled if the chemical potential of the bath changes from μ_o to $\mu_{ext} < \mu_o$ and the gel shrinking is measured by the change in volume (from the dry state) known from equation (.1) with μ_o changed in μ_{ext} . For $\mu_{ext} = -0.123$ J/mol, we get $J = 38.8$, corresponding to halving the initial \mathcal{S}_o volume, and thus releasing a liquid volume equal to 38.8 times the dry volume V_d . It is worth noting that: (i) for $\mu_o \simeq 0$ ($1/\mu_o \simeq 0$), any small variations in the chemical potential determine high (small) changes in volume; (ii) these latter are driven by changes in the chemical potential of the bath which enter the model via chemical boundary conditions. Alternatively, the liquid content in passive gels can be changed by loading gels on their boundary¹⁸.

In the following, we shall show how an active gel can achieve a same de-swelling, remaining at constant the chemical potential, but shortening the mean free length of the polymer meshwork.

As a difference, the state of an active gel can be driven by bulk through the action of inner (molecular) motors and the amount of energy required to attain the thermodynamical equilibrium state \mathcal{S} under the same bath ($\mu_{ext} = \mu_o$) can be quantified through our model. Besides, it can describe the dynamics of liquid redistribution within the swollen state \mathcal{S}_o under not uniform bulk actions in presence of impermeable boundaries (see figures 4-5).

The chemo-mechanical state of an active gel sphere is described by the radial displacement $u = u(r, t)$ from the dry state ([m]) and the liquid concentration $c = c(r, t)$ per unit of dry volume ([mol/m³]), as for passive gels, plus the remodeling variables $\gamma_r = \gamma_r(r, t)$ and $\gamma_\theta = \gamma_\theta(r, t)$ which describe the radial and hoop macroscopic changes in length of the sphere due to network remodeling. The chemo-mechanical state of the active gel sphere is ruled by the balance of forces and liquid mass

$$\sigma'_r + \frac{2}{r}(\sigma_r - \sigma_\theta) = 0 \quad \text{and} \quad \dot{c} = -(h' + \frac{2}{r}h), \quad (.2)$$

where σ_r and σ_θ are the radial and hoop components of the dry-reference stress and h is the radial liquid flux. Moreover, the active gel sphere has two more balance laws¹⁹

$$m \frac{\dot{\gamma}_r}{\gamma_r} = \beta_r - E_r \quad \text{and} \quad m \frac{\dot{\gamma}_\theta}{\gamma_\theta} = \beta_\theta - E_\theta, \quad (.3)$$

showing that the evolution of γ_r and γ_θ is driven by the difference between the radial and hoop components β_r and β_θ ($[J/\text{m}^3]$) of the remodeling bulk source and the corresponding Eshelby components E_r and E_θ ($[J/\text{m}^3]$)^{4,16,17}, and depends on the resistance to remodeling m ($[m] = J \text{ s/m}^3$). The evolution of γ_r and γ_θ depends on the remodeling sources and on the resistances to mobility m , which we assumed equal in the radial and hoop direction. A characteristic remodeling time τ_r is naturally identified by the ratio between m and the intensity of the remodeling sources: $\tau_r = \min(m/|\beta_r|, m/|\beta_\theta|)$. For active gels, the change J of volume due to swelling is equal to the liquid uptake or release up to the change $J_a = \gamma_r \gamma_\theta^2$ of the gel volume due to remodeling

$$J = J_a + \Omega c. \quad (.4)$$

Equation (.4) dictates that liquid uptake locally determines the change of volume from the remodeled state to the actual state (see figure 1). It also holds $J = \lambda_r \lambda_\theta^2$ with the radial and hoop deformations $\lambda_r = 1 + u'$ and $\lambda_\theta = 1 + u/r$, measured from the dry state.

Thermodynamically consistent constitutive equations for σ_r and σ_θ , h , E_r and E_θ , and the chemical potential μ of the liquid within the gel are derived from a revisited Flory Rehner free-energy

$$\psi = J_a(\varphi_e + \varphi_m) - p(J - (J_a + \Omega c)) \quad (.5)$$

per unit dry volume, additively split into the elastic component φ_e and the mixing component φ_m per unit remodeled volume, and accounting for the volumetric constraint (.4) maintained by the reaction p .²⁰ The elastic component φ_e has a neo-Hookean form and depends on the effective radial and hoop strains λ_r/γ_r and $\lambda_\theta/\gamma_\theta$, respectively²¹:

$$\varphi_e = \frac{G}{2} J_a \left((\lambda_r/\gamma_r)^2 + 2 (\lambda_\theta/\gamma_\theta)^2 - 3 \right). \quad (.6)$$

The mixing component φ_m depends on the *polymer fraction* ϕ , a key chemical variable, which is given by

$$\phi = \frac{J_a}{J} = \frac{J_a}{J_a + \Omega c} = \frac{1}{J_e}, \quad \text{where } J_e = \frac{J}{J_a}, \quad (.7)$$

and takes the following form

$$\varphi_m = \frac{RT}{\Omega} ((J_e - 1) \log(1 - 1/J_e) + \chi (1 - 1/J_e)), \quad (.8)$$

which is formally analogous to the standard Flory-Rehner mixing energy, proviso J_e is replaced by $1/\phi$. However, from the point of view of macroscopic mechanics, it is quite different as here polymer fraction is not related to the visible change of volume J (see equations (.4) and (.7)). Standard constitutive procedures yields:

$$\sigma_r = G \lambda_r \frac{\gamma_\theta^2}{\gamma_r} - p \lambda_\theta^2 \quad \text{and} \quad \sigma_\theta = G \lambda_\theta \gamma_r - p \lambda_r \lambda_\theta; \quad (.9)$$

$$\mu = RT \left(\log \frac{J_e - 1}{J_e} + \frac{1}{J_e} + \frac{\chi}{J_e^2} \right) + p \Omega, \quad (.10)$$

$$h = -\frac{Dc}{RT \lambda_r^2} \mu', \quad (.11)$$

with D the diffusivity parameter ($[D] = \text{m}^2/\text{s}$). The dynamics described by the equation (.2)₂ introduces the characteristic diffusion time $\tau_d = l^2/D\varepsilon$ into the model, where l is a characteristic diffusion length and $\varepsilon = G\Omega/RT$ measures the ratio between the elastic and the mixing energy. Finally, the radial and hoop Eshelby components are:

$$E_r = \psi - \lambda_r \sigma_r + -c \mu, \quad E_\theta = \psi - \lambda_\theta \sigma_\theta - c \mu. \quad (.12)$$

For a given μ_o , the stress-free solution J_o of (.1) is also a steady solution if $J_a = 1$ and (.3) yields $\dot{\gamma}_r = \dot{\gamma}_\theta = 0$; this second requirement implies that the resistance to mobility m be infinite, or that $\beta_r = E_r$ and $\beta_\theta = E_\theta$. It means that for active gels, a remodeling source is required to maintain the thermodynamic equilibrium at \mathcal{S}_o (unless $m \rightarrow \infty$)^{5,6}. Thus, at \mathcal{S}_o , we have $\sigma_r = \sigma_\theta = 0$ and $\mu = \mu_o = 0$ to fulfill the stress-free condition, and $E_r = E_\theta = \beta_r = \beta_\theta = \beta_o = \psi_o$ for the steadiness, with ψ_o the amount of energy per unit dry volume required to attain the thermodynamical equilibrium. In the present case, we get $\beta_o = -8 \cdot 10^7 \text{ J/m}^3$.

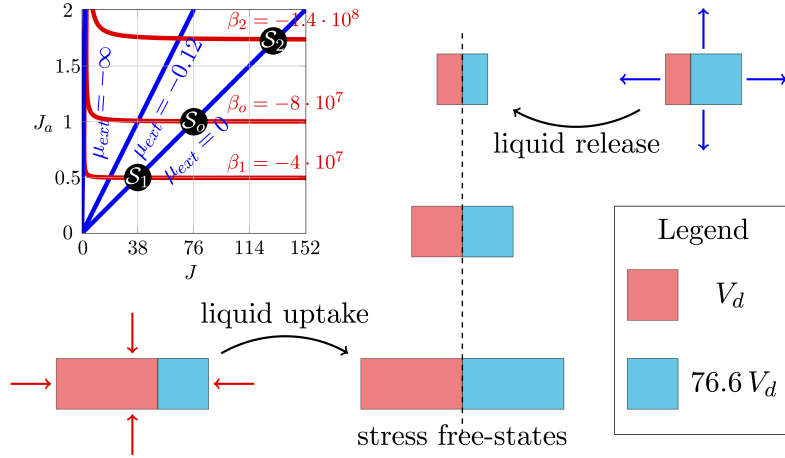


Figure 2. Activation-induced liquid release and uptake. Top left) State space (J, J_a) ; the intersections between iso- μ_{ext} (blue) and iso- β (red) represent states that are both stress-free and steady. The three highlighted states \mathcal{S}_i refer at our example: starting from \mathcal{S}_o , it is possible to halve the volume and get \mathcal{S}_1 by increasing β ; analogously, by decreasing β the volume can double to \mathcal{S}_2 . All the states along the blue line μ_{ext} have the same value $J_{eo} = 77.6$. Center) The three states \mathcal{S}_i are shown in a stack, with cartoons representing polymer in red and liquid in cyan (volumes not in scale); the middle cartoon represents \mathcal{S}_o , with $J_a = 1$ and $J = J_{eo} J_a = 77.6$; above we have \mathcal{S}_1 , with $J_a = 0.5$ and $J = J_{eo} J_a = 38.8$; below we have \mathcal{S}_2 , with $J_a = 2$ and $J = J_{eo} J_a = 155.2$. Top right) Contracted swollen polymer with $J_a = 0.5$ and same liquid content as \mathcal{S}_o : as $J_e > J_{eo}$, this state is under tension and liquid must be released. Bottom left) Expanded swollen polymer with $J_a = 2$ and same liquid content as \mathcal{S}_o : as $J_e < J_{eo}$, it is under compression and liquid must be absorbed.

The remodeling source is a further control of the state of the system: fixed $\mu_{\text{ext}} = \mu_o$, it is possible to induce a liquid release or uptake by changing the value of β . Following our example, to $\beta_1 = \beta_o + \Delta\beta$, with $\Delta\beta = 4 \cdot 10^7 \text{ J/m}^3$, there correspond a different stress-free and steady state \mathcal{S}_1 , having $J_a = 0.5$; it follows a halving of the initial volume, that is, $J = J_o J_a = 38.8$ times the dry volume V_d . It is worth confronting this result with the aforementioned one for passive gel, where the halving of the volume has been induced by lowering μ_{ext} .

By contrast, for a $\Delta\beta < 0$, we get a volume increase, as shown in figure 2. It is worth noting that the final state only depends on $\Delta\beta$, but the time evolution of the state variables is related to the time τ_β required to switch from β_o to β_1 .

The dynamics from \mathcal{S}_o to \mathcal{S}_1 is ruled by the equations (.2)-(.3), and the results corresponding to $\tau_\beta = 100 \text{ s}$, $m = 10^5 \text{ Pa/s}$, $D = 10^{-3} \text{ m}^2/\text{s}$, and a sphere of dry radius $r_d = 1 \text{ mm}$, are described in figure 3. Panel (a) shows the local volume change J versus the dimensionless radius r/r_d (orange dashed lines), at three times t_i ; the corresponding liquid distribution is shown in the bottom panel (c). At $t_2 = 100 \text{ s}$, with $t_2 > \tau_d \simeq 10^1 \text{ s} \gg \tau_r = 10^{-3} \text{ s}$, the liquid has already been completely expelled from the periphery of the sphere, where $J = 38.8$, whereas in the core it still takes the initial value J_o .

The trajectory of the mean values \bar{J} , \bar{J}_a of the volume ratios can be illustrated in the contraction-swelling diagram of axes J/J_o and J_a in panel (b). As stresses are zero and $\mu = \mu_o$ at both \mathcal{S}_o and \mathcal{S}_1 , J_e takes the same value at the two states (see also figure 2).

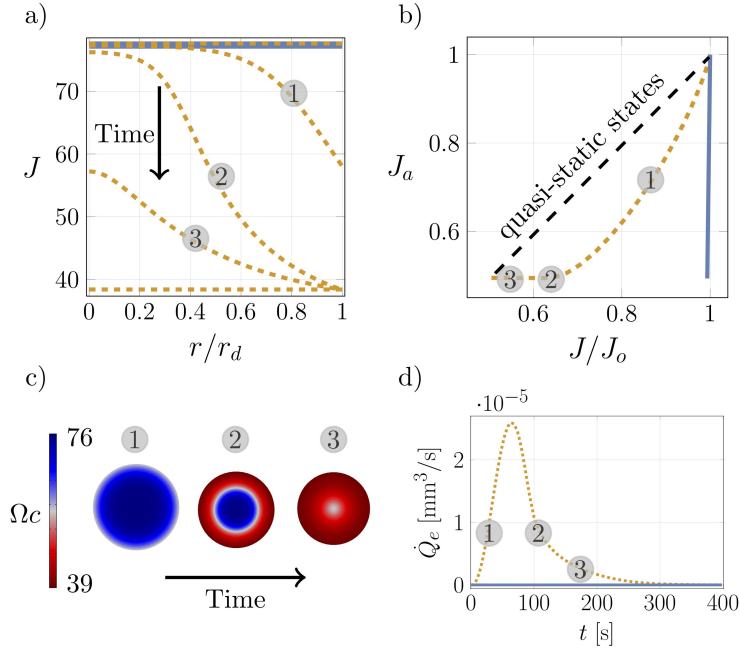


Figure 3. Contraction of a permeable spherical gel. (a) Swollen volume ratio J versus dimensionless radius r/r_d (dashed orange line) at three instants during time evolution; deswelling starts at the boundary and becomes uniform at steady state; $t_1 = 50$ s, $t_2 = 100$ s, $t_3 = 150$ s. (b) Trajectory of the point $(\bar{J}(t)/J_o, \bar{J}_a(t))$ (dashed orange line) in the $(J/J_o, J_a)$ plane; the dashed black line represents the stress-free states. (c) Liquid content at the three instants of panel (b). (d) Liquid flux: after the initial peak it decreases until the steady value is attained, when liquid flux is null. The case of the impermeable sphere is also shown in blue solid lines.

Hence, as $J_e = J_o$ at \mathcal{S}_o where $J_a = 1$ and $J = J_o$, the point $(1, 1)$ in the diagram marks \mathcal{S}_o ; at any other equilibrium state, $J_e = J_o = J/J_a$. It identifies the bisectrix of the diagram (dashed black line) as the locus of the stress-free states. So, the trajectory of \bar{J} and \bar{J}_a starts and ends on the line and is far from it along the transient (orange dashed lines). Finally, the liquid flux $\dot{Q}_e = \Omega h$ ($[\dot{Q}_e] = \text{mm}^3/\text{s}$) (panel d) shows a pattern similar to the one already evidenced when contraction of swollen active soft matter is involved^{5,6,22}, with a peak at the first times and slowly decreases to zero.

When the boundary of the swollen sphere is made impermeable, liquid is exchanged with the environment and J changes only because of the contraction J_a , see blue solid lines in top panels of figure 3. The trajectory of the mean values \bar{J} , \bar{J}_a is almost vertical (panel b), and ends at a highly stressed state. To get liquid migration within the swollen state \mathcal{S}_o , a not uniform bulk active source is required.

In particular, we study liquid migration as consequence of a stepwise constant remodeling source which segregates the sphere into an active and a passive region where $\beta > \beta_o$ and $\beta = \beta_o$, respectively. We consider both a core activation and a peripheral activation: $\beta = \beta_o + \Delta^c$ in the core region $0 \leq r/r_d < r_c = 0.4$ and $\beta = \beta_o$ otherwise, $\beta = \beta_o + \Delta^p$ in the peripheral region $0.6 = r_p \leq r/r_d \leq 1$ and $\beta = \beta_o$ otherwise, respectively. The intensities Δ^c and Δ^p are chosen in such a way to have the same amount of energy $\Delta^c V_c = \Delta^p V_p = 0.012$ J, with $V_c = 4/3\pi r_c^3$ and $V_p = 4/3\pi(r_d^3 - r_p^3)$. Our results, summed up in figures 4-5, allow to discuss the interaction between liquid migration and stress generation in the dynamics of active gels.

The starting point of the analysis is \mathcal{S}_o and we assume that the dry sphere swelled and only later its boundary was made impermeable so that the uptaken liquid is trapped into \mathcal{S}_o forever. At \mathcal{S}_o , the liquid volume V_{l_o} is $J_o V_d = 3.25 \cdot 10^{-7} \text{ m}^3$ and the steady state is maintained by the bulk source β_o . Any change ΔV_l in the liquid volume from V_{l_o} is due to

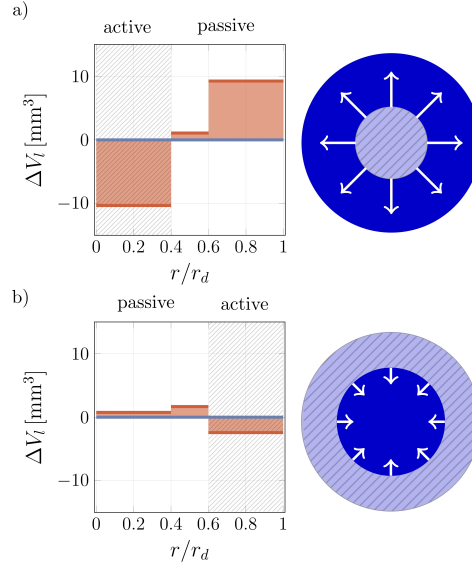


Figure 4. Contractile activation of the impermeable spherical gel. Left panels show the volumes of liquid which are displaced due to activation: initial liquid distribution (blue line), final average liquid content (red line); the orange areas show the volume ΔV_l of liquid that has migrated. Right panels show the active regions (light blue) and the passive regions (dark blue) in the sphere. Arrows denote liquid flux from the active contracted region to the passive one.

the successive increases in the remodeling source.

Figure 4 shows the initial, uniform liquid distribution in the $r/r_d - \Delta V_l$ plane as a blue solid line ($\Delta V_l = 0$). Red lines denote the average liquid content at the final state, in the core and in the intermediate and peripheral regions; thus, the orange areas represent the volume of liquid which has migrated. When the core is activated (top), a large volume of liquid migrates from the core, where $\Delta V_l < 0$, to the periphery where $\Delta V_l > 0$, with an almost negligible change of the liquid content in the intermediate region. On the contrary, in the case of peripheral activation of equal global intensity and hence smaller density, a small migration towards the core is realized, which mainly involves both the intermediate region and the core. The cartoon on the right depict active regions in light blue and passive regions in dark blue; arrows denote liquid flux from the active to the passive regions.

The model allows to look at the pattern over time of the radial and hoop remodeling variables γ_r and γ_θ in two points at the interface between active and passive regions: one inside the core (figure 5, left panel) and one outside the core (figure 6, right panel). They describe the macroscopic changes in length of the sphere due to network remodeling and are not visible unless they are realized and take the values λ_r and λ_θ of the radial and hoop deformations. In this case, it would hold $J_a = J$, no changes in the liquid concentration would occur (see equation (.4)) and stresses would be zero. The liquid content of the sphere makes this situation unrealizable: material remodeling determines liquid migration which is coupled to the stress state in the sphere.

The patterns $\gamma_r(t)$ and $\gamma_\theta(t)$ are driven by the equations (.3) and (.12) and, due to the isotropic mobility and activation source and granted for the representation form of the Eshelby components, may differ one from each other only for the $\lambda_r \sigma_r$ and $\lambda_\theta \sigma_\theta$ components in the equations (.12). Inside the active core, due to the difference between remodeling and diffusion characteristic times ($\tau_r \simeq 10^{-3}$ s $\ll \tau_d \simeq 10$ s) and being $\tau_r \ll \tau_\beta$ with $\tau_\beta = 1$ s, or 100 s, before diffusion starts γ_r and γ_θ are strongly driven by the increase $\Delta^c(t)$ in the activation source, and take their steady values when $\Delta^c = \Delta^c(t_\beta)$. Moreover, when diffusion starts liquid starts being released from the core so driving a negative radial stress and a positive hoop stress which determine the characteristic patterns observed in figure 5,

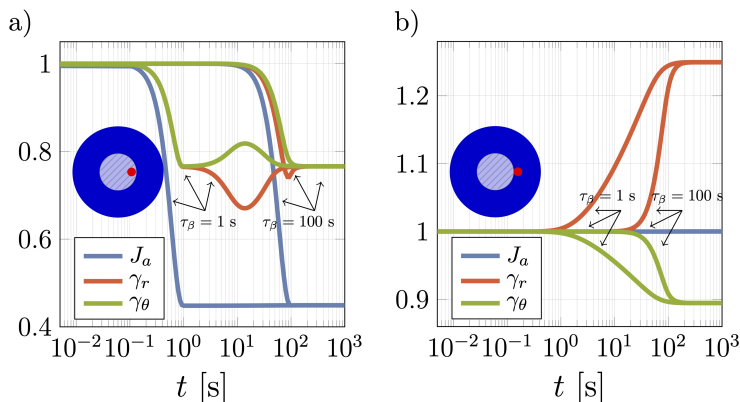


Figure 5. Radial γ_r and hoop γ_θ remodeling components (orange and green lines, respectively) and J_a (blue lines) over time in two selected points (red points) inside (panel a) and outside (b) the active core region due to an increase in the remodeling external source which takes the value Δ^c in a time $\tau_\beta = 1$ s and $\tau_\beta = 100$ s.

which disappear when τ_d is over. These behaviours are more evident for fast ($\tau_\beta = 1$ s) than for slow ($\tau_\beta = 10^2$ s) activation sources.

Actually, figure 5 also records $J_a = \gamma_r \gamma_\theta^2$ over time which delivers changes in volume due to activation. It confirms that the remodeling-induced change in the gel volume in the active core is very fast and we can observe an almost direct relationship between $\Delta^c(t)$ and $J_a(t)$ which takes its steady value $J_a \approx 0.5$ in the time τ_β . This value is unchanged by diffusion, due to commented above changes in γ_r and γ_θ induced by diffusion.

On the other hand, in the passive region before diffusion starts remodeling is absent and both the components γ_r , γ_θ and J_a keep the unit value. When diffusion starts, due to the activation of the core, liquid starts migrating from the core to the periphery, also remodeling starts and γ_r and γ_θ take different patterns: a radial expansion up to $\gamma_r \approx 1.25$ and a hoop contraction up to $\gamma_\theta \approx 0.9$, corresponding to a positive radial stress and a negative radial stress, as it is expected in a region whereas liquid has been uptaking.

The values taken by γ_r and γ_θ at the steady stress-free state are shown in the left panel of figure 6 (top), together with the remodeling of four volume elements along the radius of the sphere (bottom) for $\tau_\beta = 100$ s. In the core region, volume elements are isotropically contracted (point 1); at the interface, the difference between γ_r and γ_θ makes the contraction of the volume element highly anisotropic (point 2); after the peak, the anisotropy of the contraction reduces moving towards the boundary (point 3) up to a minimum value at point 4. At the interface, as also shown by figure 5, radial remodeling quickly changes from contraction (in the core) to expansion (in the periphery). As it corresponds to a stress-free state, it can be easily shown from equations (.9) that γ_r and γ_θ also defines the visible radial and hoop deformations λ_r and λ_θ up to a common multiplier. Hence, as expected, figure 6 reveals that at the interface sphere deformation is anisotropic and corresponds to a radial contraction/expansion at the active/passive region whereas it moves towards isotropy at the boundary. The hoop stress σ_θ evolves in time (see figure 6, right top panel) to accomodate liquid migration which after a time $t_2 > \tau_d$ has decreased significantly, as shown in figure 6, see panel (d).

In summary, bulk contraction can be modulated to get liquid migration and material and geometrical parameters can be tuned to realize fast contraction and delayed liquid migration.

The model is able to describe different phenomena where water motion and growth or contraction of a solid are involved. The present study delivers a deep insight into processes that can take place in natural elements, such as cells, but also in synthetic active gel system. The results for an impermeable gel sphere demonstrate that the migration of liquid, which is essential in biological organisms and tissues, is strongly coupled with remodeling actions. The latter, are necessary not only to relax stresses but also to induce a change of the body shape which is often observed in natural systems. Moreover, we also show as differential

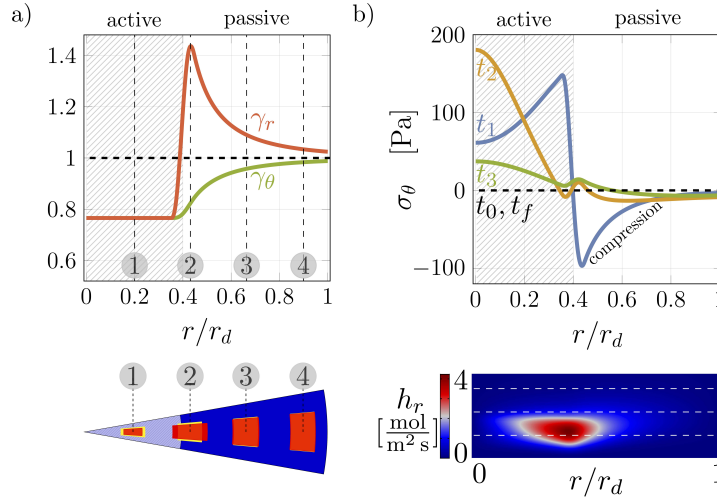


Figure 6. Remodeling components at steady final state and stress dynamics for the active core case corresponding to $\tau_\beta = 100$ s. a) Top: remodeling components γ_r, γ_θ at steady final state have same value in the active region, fully isotropically contracted, while have different values in the passive region. Bottom: cartoon with four spherical volume elements at initial and final state, respectively yellow and red colored. The shape change of the volume element due to remodeling processes are necessary to realize a stress-free final state. b) Top: High stresses are reached firstly close to the active/passive interface (time $t_1 = 50$ s), then higher stresses move towards the center (times $t_2 = 100$ s and $t_3 = 150$ s). Black dashed line represents the initial and final state which are stress-free. Bottom: flux over time is high close to the interface while is low at the center nevertheless high stresses are reached at same instants.

growth/contraction patterns are realized both in regions where gel is activated but also where liquid migrates. This observation opens new possibilities to predict the biological behavior in cells and tissues where high stresses can lead to disruptive processes at micro and macro scale.

This work is supported by MIUR (Italian Minister for Education, Research, and University) through *PRIN 2017, Mathematics of active materials: From mechanobiology to smart devices*, project n. 2017KL4EF3.

REFERENCES

- ¹E. Moeendarbary, L. Valon, M. Fritzsche, A. R. Harris, D. A. Moulding, A. J. Thrasher, E. Stride, L. Mahadevan, and G. T. Charas, “The cytoplasm of living cells behaves as a poroelastic material,” *Nature Materials* **12**, 253–261 (2013).
- ²J. Prost, F. Julicher, and J.-F. Joanny, “Active gel physics,” *Nature Physics* **11**, 111 – 117 (2015), mechanics of Rubber - in Memory of Alan Gent.
- ³M. H. Armstrong, A. Buganza Tepole, E. Kuhl, B. R. Simon, and J. P. Vande Geest, “A finite element model for mixed porohyperelasticity with transport, swelling, and growth,” *PLOS ONE* **11**, 1–35 (2016).
- ⁴M. Curatolo, S. Gabriele, and L. Teresi, “Swelling and growth: a constitutive framework for active solids,” *Meccanica* **52**, 3443–3456 (2017).
- ⁵M. Bacca, O. A. Saleh, and R. M. McMeeking, “Contraction of polymer gels created by the activity of molecular motors,” *Soft Matter* **15**, 4467–4475 (2019).
- ⁶M. Curatolo, P. Nardinocchi, and L. Teresi, “Dynamics of active swelling in contractile polymer gels,” *Journal of the Mechanics and Physics of Solids* **135**, 103807 (2020).
- ⁷J. H. Kroeger, R. Zerzour, and A. Geitmann, “Regulator or driving force? the role of turgor pressure in oscillatory plant cell growth,” *PLOS ONE* **6**, 1–12 (2011).
- ⁸L. Beuzamy, N. Nakayama, and A. Boudaoud, “Flowers under pressure: ins and outs of turgor regulation in development,” *Annals of Botany* **114**, 1517–1533 (2014), <https://academic.oup.com/aob/article-pdf/114/7/1517/16993167/mcu187.pdf>.
- ⁹M. Sahaf and E. Sharon, “The rheology of a growing leaf: stress-induced changes in the mechanical properties of leaves,” *Journal of Experimental Botany* **67**, 5509–5515 (2016), <https://academic.oup.com/jxb/article-pdf/67/18/5509/18087327/2485673.pdf>.

- ¹⁰D. Zhang and B. Zhang, “Pectin drives cell wall morphogenesis without turgor pressure,” *Trends in Plant Science* (2020), <https://doi.org/10.1016/j.tplants.2020.05.007>.
- ¹¹F. Xu, C. Fu, and Y. Yang, “Water affects morphogenesis of growing aquatic plant leaves,” *Phys. Rev. Lett.* **124**, 038003 (2020).
- ¹²C. Fei, S. Mao, J. Yan, R. Alert, H. A. Stone, B. L. Bassler, N. S. Wingreen, and A. Košmrlj, “Nonuniform growth and surface friction determine bacterial biofilm morphology on soft substrates,” *Proceedings of the National Academy of Sciences* **117**, 7622–7632 (2020), <https://www.pnas.org/content/117/14/7622.full.pdf>.
- ¹³P. J. Flory and J. Rehner, “Statistical mechanics of cross-linked polymer networks i. rubberlike elasticity,” *J Chem Phys* **11**, 512–520 (1943).
- ¹⁴P. J. Flory and J. Rehner, “Statistical mechanics of cross-linked polymer networks ii. swelling,” *J Chem Phys* **11**, 521–526 (1943).
- ¹⁵E. K. Rodriguez, A. Hoger, and A. D. McCulloch, “Stress-dependent finite growth in soft elastic tissues,” *Journal of Biomechanics* **27**, 455 – 467 (1994).
- ¹⁶A. DiCarlo and S. Quilgotti, “Growth and balance,” *Mechanics Research Communications* **29**, 449–456 (2002).
- ¹⁷M. E. Gurtin, *Configurational Forces as Basic Concepts of Continuum Physics* (Springer, 2000).
- ¹⁸P. Nardinocchi and L. Teresi, “Actuation performances of anisotropic gels,” *Journal of Applied Physics* **120**, 215107 (2016).
- ¹⁹See^{4,6} for further details.
- ²⁰The Jacobians J_a and J have a key role in changing volume-elements. Precisely, let dV_d , dV_a , and dv be the dry-reference, the remodeled, and the actual volume-elements, respectively. Then, they are related by the Jacobians as

$$dV_a = J_a dV_d \quad \text{and} \quad dv = J dV_d = \frac{J}{J_a} dV_a. \quad (.13)$$

In these terms, equation (.4) can be rewritten as

$$dv = dV_a + dV_{\text{sol}}, \quad (.14)$$

with $dV_{\text{sol}} = \Omega c dV_d$ denoting the liquid volume-element. So, using these volume relationships, free energies per unit remodeled volume as φ_e and φ_m are transformed into free energies per unit dry volume as $\psi dV_d = (\varphi_e + \varphi_m) dV_a = J_a(\varphi_e + \varphi_m) dV_d$.

²¹An effective strain measures a change in length from the remodeled state.

²²Y. Ideses, V. Erukhimovitch, R. Brand, D. Jourdain, J. Salmeron, Hernandez, U. Gabinet, S. Safran, K. Kruse, and A. Bernheim-Groswasser, “Spontaneous buckling of contractile poroelastic actomyosin sheets,” *Nature Communications* **9**, 2461 (2018).